NUMERICAL ANALYSES OF COLD-FORMED THIN-WALLED SECTIONS WITH CONSIDERATION OF IMPERFECTIONS DUE TO THE PRODUCTION PROCESS

Albrecht Gehring [1] and Helmut Saal [2,*]

[1] *Research assistant, Versuchsanstalt für Stahl, Holz und Steine, Universität Karlsruhe (TH), Germany*
[2] *Professor, Versuchsanstalt für Stahl, Holz und Steine, Universität Karlsruhe (TH), Germany*
*(Corresponding author: E-mail: helmut.saal@va.uka.de)

ABSTRACT: The load bearing capacity of cold-formed thin-walled sections strongly depends on deviations from the nominal dimensions and the material properties. The former reduce the load bearing capacity. The latter enhance the load bearing capacity, because of work hardening during the manufacturing process. It is difficult to realistically account for both effects in a finite-element analysis of the load bearing capacity of thin-walled sections. Today, cost intensive testing is necessary, if a maximum utilization of the load bearing capacity is desired. The properties of a product can be determined during the product development process with a new simulation strategy, which covers the production process as well as the state of serviceability of a product. The roll forming process is simulated first followed by a non-linear ultimate limit state analysis. The combination of both analysis steps gives the possibility to determine the load bearing capacity realistically as deviations from the nominal value of dimensions and material properties areincluded in the analysis. The new analysis strategy is demonstrated for a U-section with respect to different aspects concerning work hardening and the load bearing capacity of a C-section. It is shown, that the new strategy leads to a realistic estimation of the load bearing capacity of thin gauged sections.

Keywords: Numerical analyses, cold-formed sections, imperfections, work hardening, ultimate limit state

1.   INTRODUCTION

Cold-formed thin-walled sections are produced by roll forming. Roll forming is a technology where a flat strip is formed into a cross-section continuously. The process involves a progressive bending of the metal strip as it passes through a series of forming tools, see Figure 1. The design of the rolling schedule is done by unfolding the profile. From this, the flower diagram is obtained, see Figure 1. Different calibration methods are used to obtain the flower diagram. Arc bending or the constant radius method are in common use, but other methods are also applied, Halmos [1], Bogojawlenski et al [2]. The sheet is deformed by an intended transversal bending load and unavoidable reversed bending and shear loads in longitudinal and transverse direction during roll forming. The latter arise from the curvature of a fiber during the forming process and they significantly influence the forming process and the final shape of the cross-section, Halmos [1], Bogojawlenski et al [2].
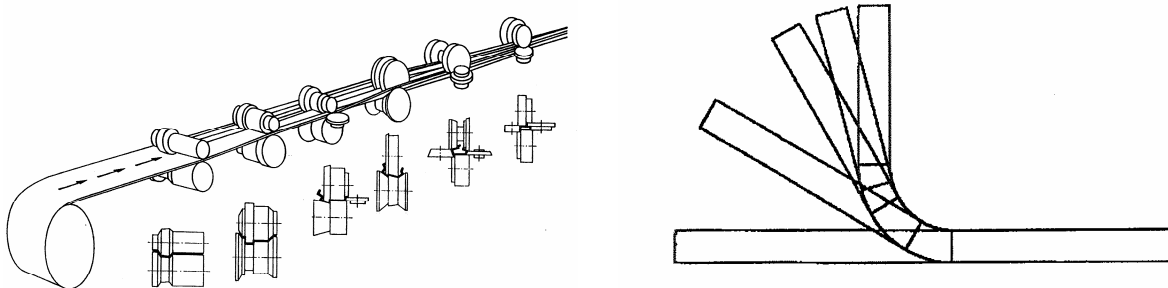

Figure 1. Roll Former (Left); Flower Diagram of a U-Profile (Right)

2.   FINITE ELEMENT MODEL

2.1   General Considerations

The roll forming process can be regarded as a quasi-static dynamic process. Thus an explicit solver is applicable. The explicit solver is advantageous in an analysis, where contact is involved, Abaqus [3]. An implicit solver is used for subsequent springback analyses. The software package Abaqus [4] is used for all analyses jobs. The analyses are executed parallel with the domain-level method. The analyses jobs are run mainly on 4 cpus or 8 cpus on the HP XC 6000 cluster and on HP XC 4000 cluster of the Universität Karlsruhe [5].

2.2   Model Details

The forming tools are represented as rigid bodies in all analyses. The blank is meshed with the 4 node shell element S4R. In the flat areas an element size of 3 x 3 mm with 5 integration points through thickness are used and in the bending area an element size of 1 x 3 mm with 9 integration points through thickness are used. The ends of the sheet are constrained in rolling direction to simulate an endless sheet. Fixed boundary conditions are applied on the forming tools in all analysis jobs. The general contact algorithm is used in the analysis, as no restrictions are placed on the domain decomposition for domain-level parallelization. Friction is neglected with all analyses. The load is applied as velocity in rolling direction. The velocity is increased in the first 0.05 s from zero to a constant forming speed using the smooth step definition of ABAQUS [4] to minimize inertia effects in this quasi-static analysis. Through this, longitudinal oscillations of the sheet are minimized and thus the probability to induce numerically noisy or inaccurate results is reduced. The verification of the model is described in detail by Gehring and Saal [6].

2.3   Material Model

A Young's Modulus of E = 210 GPa and a Poisson's ratio of ν = 0.3 define the elastic response in all analyses. The plastic part is described by the following material models, Khan and Huang [7]:

- Standard isotropic hardening with von Mises type yield function and associated plasticity
- Yield function according to the Hill stress potential and associated plasticity

In all models, the isotropic hardening behaviour of the material is modelled with the modified Ludwik-Hollomon equation, which is usually applied in forming analysis, Lange [8]. In this Equation

$$k_f(\varepsilon_p) = f_y \cdot \Phi \cdot \left(\frac{e}{n}\right)^n \cdot \varepsilon_p^n \tag{1}$$

f_y is the yield strength, Φ is the strength ratio of tensile strength to yield strength, ε_p are true plastic strains, e is the Euler number and n is a constant. Eq. 1 gives a good approximation of the flow curve for low alloy steel and aluminium alloys, if the exponent n is related to the uniform elongation ε_u in terms of n = ln (1+ ε_u), Lange [8]. The Hill stress potential is expressed as

$$f(\sigma) = \sqrt{F(\sigma_{22} - \sigma_{33})^2 + G(\sigma_{33} - \sigma_{11})^2 + H(\sigma_{11} - \sigma_{22})^2 + 2L\sigma_{23}^2 + 2M\sigma_{31}^2 + 2N\sigma_{12}^2} \tag{2}$$

where F, G, H, L, M and N are constants. These constants are defined as a function of the ratios R_{ij} of the reference stress σ_y to measured yield stress value $\overline{\sigma}_{ij}$, when σ_{ij} is applied as the only nonzero stress component, Khan and Huang [7]. Here, the 1-axis constitutes the rolling direction and the 2-axis is transverse to the direction of rolling. The 3-axis is normal to the sheet plane. The reference yield stress σ_y is determined in 1-direction and thus R_{11} becomes 1.00. Furthermore, the constants R_{33}, R_{13} and R_{23} are set to 1.00, because effects of a through-thickness anisotropy can be neglected in roll forming, Engl and Stich [9].

3.   DESIGN CONSIDERATIONS

3.1   General

The application of cold-formed sections in buildings is well established. The resistance of thin-walled sections can be determined with calculations based on the effective width approach according to international design codes, e.g. EN 1993-1-3 [10]. The application of the design codes leads to conservative resistance values. The full benefit of the cross-sectional resistance can be achieved only by cost intensive experimental investigations, e.g. according to the guidelines given in EN 1993-1-3 [10].

3.2   Increased Yield Strength

The strain distribution after roll forming of an U-section can be seen in Figure 2. The strains in the corners are clearly higher than in the flat areas of the cross-section. This means, that work hardening takes place mainly in the corner areas. Many studies have been made to utilize the enhanced material properties for design. The mechanical properties were determined by tensile tests with specimen from different parts of a profile. Also full-section tensile or compressive tests were performed to obtain specific average yield strength for design application. A comprehensive list of references is contained in Halmos [1], Bogojawlenski et al [2] and Yu [11].
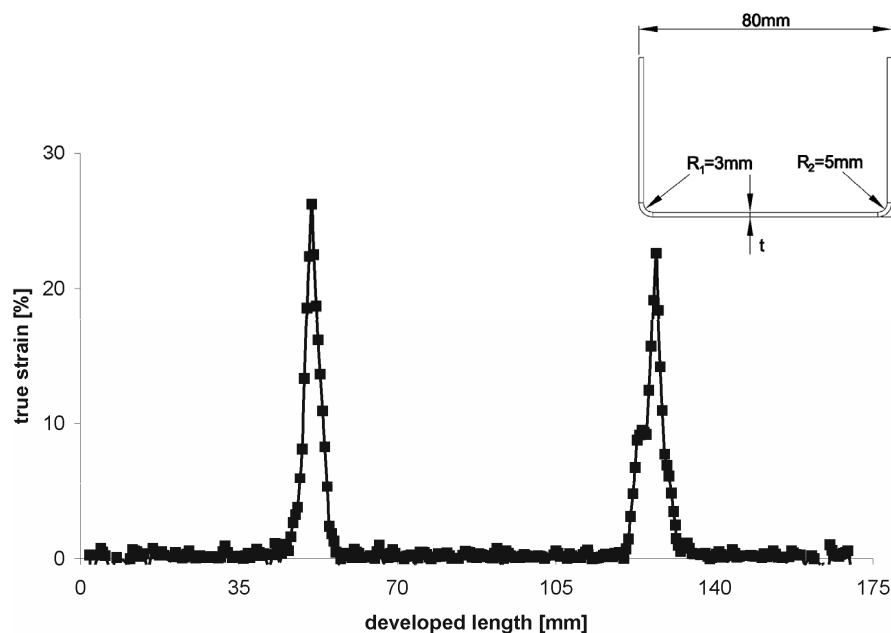

Figure 2. Strain Hardening Due to Roll Forming of a U-Section

Semi-empirical equations are introduced in international design standards for taking an enhanced yield strength into account. In EN 1993-1-3 [10], the increased yield strength f_{ya} is expressed as

$$f_{ya} = \min\left(0{,}5 \cdot \left(f_u + f_y\right); f_y + \left(f_u - f_y\right)\frac{k \cdot n \cdot t^2}{A_g}\right) \tag{3}$$

where f_y and f_u are the design values of the yield strength and the tensile strength respectively, k is a constant depending on the applied forming technology, e.g. k = 7 for roll forming, n is the number of 90° bends and A_g is the gross cross-sectional area. The increased yield strength f_{ya} is approximated in North America, Yu [11], with

$$f_{ya} = a_V \cdot f_{yc} + \left(1 - a_V\right)f_y \tag{4}$$

where f_{yc} is the corner yield strength and a_V is the ratio of corner areas to the gross cross-sectional area. The corner yield strength is calculated to

$$f_{yc} = f_y \cdot \frac{B_c}{\left(r / t\right)^m} \tag{5}$$

where

$$B_c = 3{,}69 \cdot \frac{f_u}{f_y} - 0{,}819 \cdot \left(\frac{f_u}{f_y}\right)^2 - 1{,}79$$

$$m = 0{,}192 \cdot \frac{f_u}{f_y} - 0{,}068$$

and r/t is the ratio of the bending radius to the thickness of the sheet. The application of Eq. 3 and Eq. 4 is restricted to a full effective cross-sections, certain values of the ratios r/t and f_u/f_y respectively and also to certain load cases.

3.3   Numerical Analysis

In EN 1993-1-5, Annex C [12] a guidance is given for the use of finite-element analysis for ultimate limit state verification, which includes appropriate assumptions for material models and imperfections. In the following, an analysis according to the guidance in EN 1993-1-5, Annex C [12] is called conventional analysis strategy. A non-linear finite-element analysis is necessary for the determination of the ultimate limit state of thin-walled sections. Where the non-linearity takes into account geometric deviations as well as material aspects. The imperfections can be introduced by applying equivalent geometric imperfections defined in design codes, which are scaled eigenmodes obtained from buckling analysis. Usually the material properties are assumed to be distributed uniformly, which leads to a safe estimation of the failure loads. General considerations on the characterisation of imperfections in numerical analyses are given by Schafer and Peköz [13]. Gardner and Nethercot [14] and Lecce and Rasmussen [15] introduce an enhanced yield strength due to cold-working by partitioning a cross-section. However, the problem is the lack of knowledge about the initial state of cold-formed sections, Schafer and Peköz [13].

3.4 New Analysis Approach

The properties of a roll formed section are determined with a new analysis strategy, which covers the production process as well as the state of serviceability of the section, Gehring et al [16]. The roll forming process is simulated first. This is followed by a non-linear ultimate limit state analysis. The combination of both analysis steps gives the possibility to determine the load bearing capacity realistically as deviations from the nominal value of dimensions and material properties are included in the analysis. The analysis is divided into the following steps:

- Analysis of the manufacturing process
- Introduction of imperfections and change of material properties obtained by the analysis of the manufacturing process as initial state to the new model
- Non-linear ultimate limit state analysis
- Verification of results

The new analysis strategy is demonstrated by two examples. Here, the yield strength is f_y=320MPa, the tensile strength is f_u=390 MPa and the uniform elongation is ε_u = 0.12. These values comply with steel grade S320 according to EN 10326 [17].

4. APPLICATION OF THE NEW APPROACH

4.1 Example 1: Degree of Work Hardening, Gehring and Saal [18]

Roll forming of an U 35 / 100 / 35 x 1 section is simulated. The applied inner bending radius is 4.00 mm. The profile is obtained on base of three different flower diagrams – 3 steps 30°/60°/90°, 4 steps 20°/45°/70°/90° and 5 steps 15°/35°/55°/75°/90°. The roll stands of the steps 15°, 20°, 30°, 35° and 45° are built with two tools. An additional side tool is applied in the roll stands of steps 55°, 60°, 70°, 75° and 90° respectively, see Figure 3. The inter-pass distance is set to 500 mm.
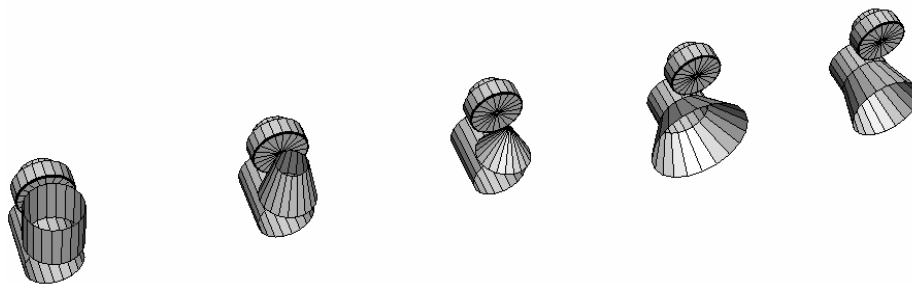

Figure 3. Roll Former with 5 Roll Stands – Steps From Right to Left: 15°/35°/55°/75°/90°

Experiments are performed to measure the effects of variables on a response. The effect of a variable means the change in the response as a variable is moved from a lower level to a higher level. Factorial designs are useful for this purpose, especially two-level factorial designs, Box et al [19]. Here, the objective is to identify the effect of mechanical material properties on the distribution of the yield stress of a roll formed section. Deviations from the assumed linear relation in two-level designs can be identified with an additional centre-point run. Then, the number m of experimental runs is

$$m = 2^k + 1 \tag{6}$$

where k is the number of variables. Here the commercial statistic software Statistica [20] is used for the design of the runs and the analysis of the results. The material properties strength ratio $\Phi = f_u/f_y$, uniform elongation ε_u and the constant R_{22} are taken as variables. The constant R_{12} is linked with R_{22} and thus not used as independent variable. On the upper level $R_{12} = 1.03$ and on the lower level $R_{12} = 1.00$. In addition the technological variable number of roll stands n_R is used. Thus, m = 17 experimental runs are necessary in this study. The experimental design can be seen in Table 1.

Plastic flow occurs in Hill's stress potential, if the equivalent yield stress according to Eq. 2 reaches the defined reference yield stress value. The size of the yield surface changes with the equivalent plastic strain ε_{eppq} isotropically. From this follows, that the yield stress $f_{y,fem}$ can be calculated with Eq. 7 and the average yield stress $f_{ya,fem}$ can be calculated with Eq. 8.

$$f_{y,fem}\left(\varepsilon_{eppq}\right) = \Phi \cdot f_y \cdot \left(\frac{e}{n}\right)^n \cdot \varepsilon_{eppq}^n \tag{7}$$

$$f_{ya,fem} = \frac{1}{l} \cdot \int_0^l f_{y,fem}\left(\varepsilon_{eppq}\right) dl \tag{8}$$

The effect of a variable on the increase of the yield strength is evaluated by statistical methods. The ratio $\psi = f_{ya,fem} / f_y$ is introduced for the evaluation. The effect C of a variable is calculated to

$$C = \frac{2}{m} \cdot \sum_{i=1}^m \left(\psi_i \cdot \{\pm\}\right) \tag{9}$$

where the subscript i refers to the run number and the sign in {} brackets to the low and high level respectively. The interaction effects are calculated similarly. Since there were no replicated runs, a standard error s_d^2 has to be estimated using higher-order interactions with negligible influence to

$$s_d^2 = \frac{1}{k} \cdot \sum_k C^2 \tag{10}$$

The significance of an effect can be identified by means of a confidence estimation based on the t distribution. Deviations from the assumed linear relations of the two-level design can be identified from the centre-point run with a curvature test. Detailed information on the statistical evaluation methods is given in Box et al [19].

The average yield stress $f_{ya,fem}$ and the maximum value of the yield stress $f_{y,fem}^{\#}$ evaluated with Eq. 7 and Eq. 8 are given in Table 1. In addition, the yield strength f_{ya} obtained from Eq. 3 and 4 are given in Table 1.

Eq. 3 leads to a safe estimation of the increased yield strength whereas Eq. 4 overestimates the increased yield strength for certain values of Φ slightly. The corner yield strength f_{yc} obtained from Eq. 5 overestimates the material response. This is evident by a comparison of f_{yc} and the individual true tensile strength $f_{u,true} = \Phi \cdot f_y \cdot (1 + \varepsilon_u)$, where f_{yc} is greater than $f_{u,true}$ for $\Phi = 1.2$ and 1.3. The distribution of the yield stress obtained from some runs with 3 roll stands are shown in Figure 4. The influence of a change of Φ and ε_u on the yield stress distribution is obvious from the web of the U-section. The steeper gradient of the flow curve with $\Phi = 1.3$ and $\varepsilon_u = 0.10$ causes more strain hardening than other combinations.

Table 1. Experimental Design and Results

Run no.	Variable [1]				Results						
	Φ	ε_u	R_{22}	n_R	$f_{y,fem}$ # [MPa]	$f_{ya,fem}$ [MPa]	ψ [-]	f_{ya} [2] [MPa]	f_{ya} [3] [MPa]	f_{yc} [4] [MPa]	$f_{u,true}$ [MPa]
1	1.10 {-}	0.10 {-}	1.00 {-}	3 {-}	389	330	1.031	323	327	403	387
2	1.30 {+}	0.10 {-}	1.00 {-}	3 {-}	459	364	1.138	328	336	510	458
3	1.10 {-}	0.15 {+}	1.00 {-}	3 {-}	386	327	1.023	323	327	403	405
4	1.30 {+}	0.15 {+}	1.00 {-}	3 {-}	455	347	1.085	328	336	510	478
5	1.10 {-}	0.10 {-}	1.05 {+}	3 {-}	390	330	1.032	323	327	403	387
6	1.30 {+}	0.10 {-}	1.05 {+}	3 {-}	460	365	1.140	328	336	510	458
7	1.10 {-}	0.15 {+}	1.05 {+}	3 {-}	388	328	1.024	323	327	403	405
8	1.30 {+}	0.15 {+}	1.05 {+}	3 {-}	462	351	1.098	328	336	510	478
9	1.10 {-}	0.10 {-}	1.00 {-}	5 {+}	386	326	1.020	323	327	403	387
10	1.30 {+}	0.10 {-}	1.00 {-}	5 {+}	459	349	1.092	328	336	510	458
11	1.10 {-}	0.15 {+}	1.00 {-}	5 {+}	381	325	1.016	323	327	403	405
12	1.30 {+}	0.15 {+}	1.00 {-}	5 {+}	451	335	1.047	328	336	510	478
13	1.10 {-}	0.10 {-}	1.05 {+}	5 {+}	390	326	1.020	323	327	403	387
14	1.30 {+}	0.10 {-}	1.05 {+}	5 {+}	457	349	1.090	328	336	510	458
15	1.10 {-}	0.15 {+}	1.05 {+}	5 {+}	382	325	1.017	323	327	403	405
16	1.30 {+}	0.15 {+}	1.05 {+}	5 {+}	453	335	1.048	328	336	510	478
17	1.20	0.125	1.00	4	420	333	1.040	325	332	460	432

[1] The + and – sign in {} brackets refer to the high and the low level respectively.
[2] According to Eq. 3
[3] According to Eq. 4
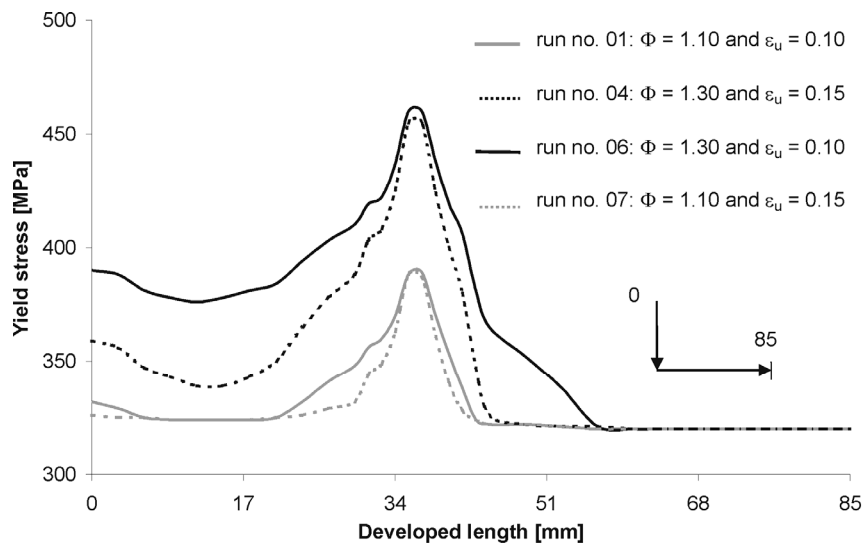[4] According to Eq. 5

Figure 4. Distribution of Yield Strength – Runs 1, 4, 6 and 7

Table 2. Statistical Evaluation

Effect [1]	$C \cdot 10^2$ [-]
Φ (1)	**6.926**
ε_u (2)	**-2.582**
R_{22} (3)	0.217
n_R (4)	**-2.795**
12	**-1.986**
13	0.162
14	**-1.818**
23	0.180
24	0.211
34	-0.203
123	0.177
124	-0.018
134	-.0188
234	-0.109
1234	-0.139

[1] Interactions are denoted with digits, e.g. the 2nd-order interaction of Φ and ε_u is denoted with 12.

The calculated effects and interactions C are given in Table 2. The comparison of the values suggests that the values in bold figures require further interpretation. All other values are supposed to be negligible and thus are used for the estimation of the standard error s_d^2, which becomes to $s_d^2 = 0.025$. From this follows the absolute value $c_{t,p}$ of a confidence interval. The values of $c_{t,p}$ on confidence levels of 95 %, 99 % and 99.9% are $c_{t,95\%} = 0.356$, $c_{t,99\%} = 0.507$ and $c_{t,99.9\%} = 0.732$ respectively.

Herewith the assumption is confirmed that the bold values are significant. The curvature test reveals, that the value of ψ does not depend linear on the variables. Thus, it is necessary to apply a higher-order statistical model for further investigations.

It is obvious that the value of the strength ratio Φ has a major effect on the increase of the yield strength.

Raising Φ from 1.1 to 1.3 leads to an increase of the average yield strength of 6.9 % in this example. The effect of ε_u is opposite to that of Φ, i.e. a smaller value of the uniform elongation ε_u results in a higher average yield strength. The increase of the yield strength decreases with increase of the number n_R of roll stands. This is due to smaller incremental bending in longitudinal direction. However, the significance of the interactions 12 and 14 shows, that the effect of the strength ratio Φ must also be considered jointly with the uniform elongation and the number of roll stands. The interaction of Φ and ε_u needs no further explanation as it was already discussed above. It is expected, that the interaction of Φ and n_R becomes less important with an increasing number of roll stands. But this has to be confirmed. It is worth to point out, that the influence of the anisotropy can be neglected.

4.2   Example 2: Load Bearing Capacity of a C-section, Gehring et al [16]

The roll forming process of a C-section 10 / 35 / 100 / 35 / 10 x 1 is simulated in the first analysis step. The applied inner bending radius is 4 mm. The C-section is obtained in 9 steps. First the edge

stiffener of the C-section is formed with 4 roll stands in steps 20°/40°/60°/90°. Then the web is folded with 5 roll stands in steps 15°/35°/55°/75°/90°. All roll stands for the stiffener and the roll stands of the steps 15° and 35° are built with two tools. An additional side tool is applied in the roll stands of steps 55°, 75° and 90° respectively. The inter-pass distance is set to 500 mm.

The second step of the analysis is to transfer the results of the preceding analysis as initial state into the new model. In this step the out-of-balance forces of the explicit analysis are removed and static equilibrium is achieved. This accounts for springback effects. Thus dimensional deviations and cold-working effects due to roll forming are considered in the initial state. The failure load is calculated in the last step of the analysis. For this, the profile is divided into 6 specimen with a length of 250 mm each. This value is less than 20 times the radius of gyration and thus agrees with the length of stub column specimen recommended in EN 1993-1-3 [10]. The virtual stub column tests are performed with the 4 specimen from the middle part of the profile. New boundary conditions are applied to the model. At one end of the sections all translation degrees of freedom are fixed and at the other end the out-of plane degrees of freedom are fixed. The sections are subjected to constant translation in longitudinal direction.

For comparison, the ultimate limit state of the C-section is determined with the conventional analysis strategy. The eigenmode which corresponds to the lowest eigenvalue is used as imperfection. The amplitude of the eigenmode is scaled to a value of b/200 which complies with the value recommended in EN 1993-1-5 [12], Annex C. The material properties are assumed to be constant across the cross-section. The boundary conditions are defined as in the last step of the advanced analysis.

Also, the effective cross-sectional area A_{eff} of the C-section is calculated in accordance with provisions given in EN 1993-1-3 [10]. The characteristic resistance $N_{c,EC3}$ of the cross-section for uniform compression according to EN 1993-1-3 [10] is

$$N_{c,EC3} = A_{eff} \cdot f_y \qquad (11)$$

The failure load N_u obtained from the finite-element analysis is calculated to

$$N_u = \sum_{i=1}^{k} n_{1,i} \qquad (12)$$

where $n_{1,i}$ is the reaction force of the i-th node in loading direction and k is the number of nodes across the section.

The variation of material properties and geometric imperfections due to the forming process is taken into account in the determination of the load bearing capacity of the 4 individual specimen. The deformed shape obtained from the new analysis exhibits typical geometric defects of roll formed sections, like the flare at the ends of the profile, see Figure 5. The geometric imperfections obtained from this analysis are shown in Figure 5, where the values are taken from a path along the arrows in Figure 5 respectively.
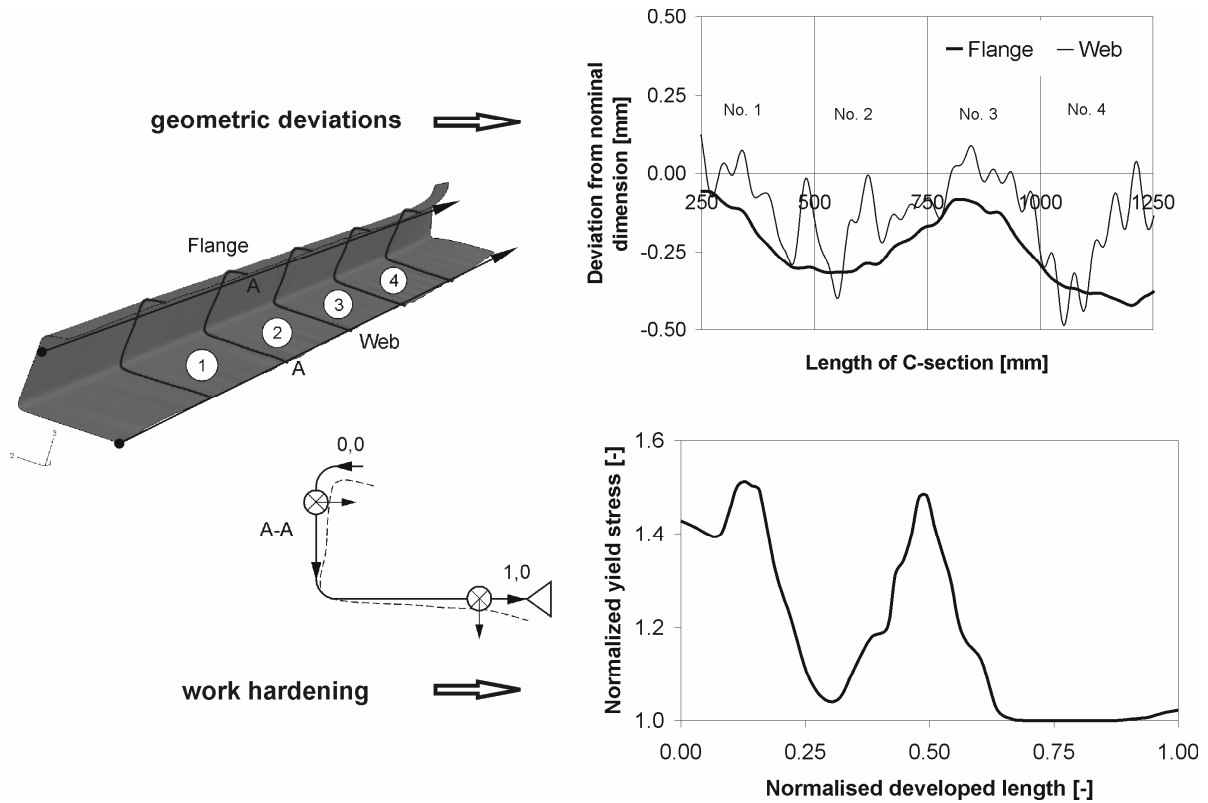
Figure 5. Predicted Imperfections from Simulation of Roll Forming Process

The numbers in Figure 5 are referring to the specimen number for the virtual stub column tests. The maximum value of the geometric imperfection of the flange is approximately 0.4 mm and of the web approximately 0.5 mm. These values agree quantitatively with measured values of similar sections, Lecce and Rasmussen [15] [16]. Also residual stresses and work hardening effects due to roll forming are considered in the initial state. The distribution of the yield stress after roll forming is shown in Figure 5. In addition, the average yield strength f_{ya} is determined according to Eq. 7 and Eq. 8.

The deformed C-sections after failure are shown in Figure 6. The failure modes deviate from each other, because the applied imperfections are different. In the conventional analysis, the wave length of the edge stiffener is longer than in the advanced analysis.

It is obvious from Figure 6, that the new analysis includes different imperfection modes and thus reveals different failure loads for each virtual test.

The failure loads determined with finite-element analyses are given in Table 3. The subscripts con and new refer to the conventional and new analysis respectively. The characteristic resistance according to EN 1993-1-3 [10] is $N_{c,EC3}$.
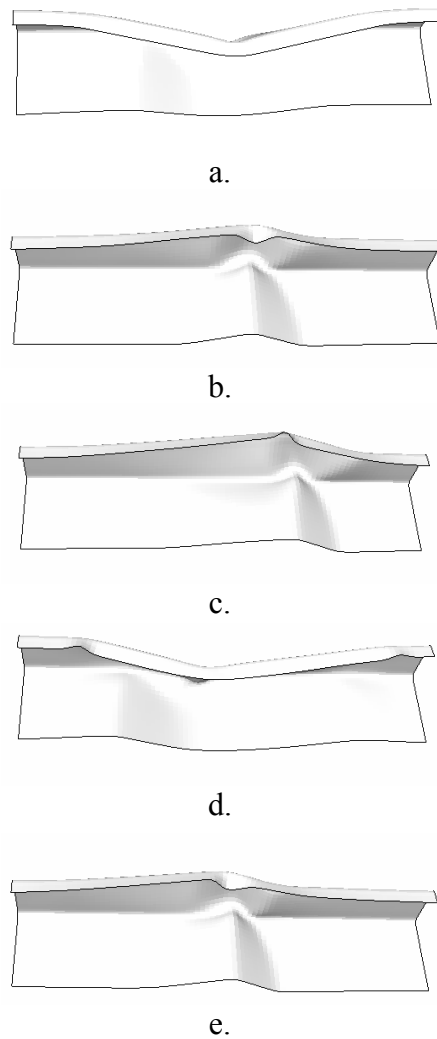
a.

b.

c.

d.

e.

Figure 6. Failed Specimen from Conventional Analysis (a.) and New Analysis (b. to e.)

Table 3. Ultimate Loads

$N_{c,EC3}$	[kN]	37,0
$N_{u,con}$	[kN]	39,8
$N_{u,new,1}$	[kN]	41,4
$N_{u,new,2}$	[kN]	42,4
$N_{u,new,3}$	[kN]	43,7
$N_{u,new,4}$	[kN]	42,4

The higher failure loads are due to the increased yield strength and the smaller geometric imperfections with the new analysis strategy. The average yield strength f_{ya} is 18 % higher than the yield strength f_y of the virgin material. The highest failure loads are obtained from the new analysis strategy. These are approximately 4 % to 10 % higher than the failure load obtained from the conventional analysis strategy and approximately 11 % to 18 % higher than characteristic resistance $N_{c,EC3}$ according to EN 1993-1-3 [10].

This example shows, that the new analysis strategy gives the opportunity to simulate the structural performance of cold-formed sections realistically. This is due to the fact, that deviations from the nominal dimensions and material properties are taken into account. The results are reasonable and

within the expected range. With this model, the effect of slight modifications of, e.g. material specification, tool design, on the failure load, can be determined easily. However, in any case the results have to be verified with some tests before introducing them as characteristic resistance values in design.

5.   SUMMARY AND CONCLUSIONS

A new simulation strategy for cold-formed thin-walled components, which covers the production process as well as the state of serviceability of a roll formed section was presented. The roll forming process is simulated first. This is followed by a non-linear ultimate limit state analysis. The combination of both analysis steps gives the possibility to determine the load bearing capacity realistically as deviations from the nominal value of dimensions and material properties are included in the analysis. The new analysis strategy is demonstrated for a U-section with respect to different aspects concerning work hardening and the load bearing capacity of a C-section. From the examples, the following conclusions can be drawn:

- The formulas for the average yield strength f_{ya} given in Eurocode 3 lead to a safe estimation of the increase of the yield stress due to roll forming.
- The strength ratio $\Phi = f_u / f_y$ is identified as the material property with the strongest influence. However, the effect of Φ interacts with the value of the uniform elongation ε_u.
- The anisotropy of the sheet material can be neglected.
- An increasing number of roll stands reduces the increase of the average yield stress.
- The enhanced average yield strength can be determined as a function of the material properties and the parameters of the roll former. This gives the opportunity to utilize the enhanced yield stress for specific sections in design.
- Deviation from the nominal dimensions and material properties are estimated realistically with the new analysis strategy and the obtained failure loads are reasonable compared to the values according to design standards.
- The characteristic resistance obtained from this process oriented analysis is higher than the characteristic values for general use in design standards.
- The new analysis strategy gives the chance to optimize the dimensions, the material specification and the manufacturing process of a section without a cost intensive experimental trial and error procedure.

It has to be kept in mind that the new analysis strategy will only lead to safe results if its application is based on a profound knowledge of the manufacturing process and the structural behaviour of the component. This demands substantial experience with experimental and numerical analysis of the object.

REFERENCES

[1]   Halmos, G.T. (Edit.), "Roll Forming Handbook", CRC Press Taylor & Francis Group, Boca Raton, 2006
[2]   Bogojawlenskij, K.N., Neubauer, A. and Ris, V.W., "Technologie der Fertigung von Leichtbauprofilen", VEB Deutscher Verlag für Grundstoffindustrie, Leipzig, 1979.
[3]   ABAQUS Documentation – Version 6.6.1, Copyright 2006, ABAQUS, Inc.
[4]   ABAQUS (Explicit & Standard); Version 6.6.1, Copyright 2006, ABAQUS, Inc.
[5]   http://www.rz.uni-karlsruhe.de/ssc/hpxc

[6]   Gehring, A. and Saal, H., "Sensitivity Analysis of Technological and Material Parameters in Roll Forming", Proceedings of the 9th International Conference on Numerical Methods in Industrial Forming Processes, Porto, 2007, pp. 781.

[7]   Khan, A.S. and Huang, S., "Continuum Theory of Plasticity", John Wiley & Sons, Inc., New York, 1995.

[8]   Lange, K. (Edit.), "Umformtechnik – Handbuch für Industrie und Wissenschaft, Band 1: Grundlagen", Berlin: Springer Verlag, 1984.

[9]   Engl, B. and Stich, G., "Neue Stahlsorten für die Kaltformung", Tagungsband 722, Studiengesellschaft für Stahlanwendung e.V., 1998.

[10]   EN 1993-1-3:2006, Eurocode 3 - Design of Steel Structures - Part 1-3: General Rules - Supplementary Rules for Cold-formed Members and Sheeting.

[11]   Yu, W.-W., "Cold-formed Steel Design", 3rd Edition, John Wiley & Sons, New York, 2001.

[12]   EN 1993-1-5:2006, Eurocode 3 - Design of Steel Structures - Part 1-5: General Rules - Supplementary Rules for Cold-formed Members and Sheeting, Annex C.

[13]   Schafer, B.W. and Peköz, T., "Computational Modeling of Cold-formed Steel: Characterizing Geometric Imperfections and Residual Stresses", Journal of Constructional Steel Research, 1998, Vol. 47, pp. 193 – 210.

[14]   Garnder, L. and Nethercot, D.A., "Numerical Modeling of Stainless Steel Structural Components – A Consistent Approach", Journal of Structural Engineering, 2004, Vol. 130, pp. 1586 – 1601.

[15]   Lecce, M. and Rasmussen, K., "Distortional Buckling of Cold-formed Stainless Steel Sections: Experimental Investigation", Journal of Structural Engineering, 2006, Vol. 132, pp. 497 – 504.

[16]   Gehring, A., Kathage, K. and Saal, H., "A New Strategy for Finite-element Analysis of the Load Bearing Capacity of Cold-formed Sections", Proceedings of the 3rd International Conference on Structural Engineering, Mechanics and Computation, Capetown, 2007, pp. 377.

[17]   EN 10326:2004, Continuously Hot-dip Coated Strip and Sheet of Structural Steels - Technical Delivery Conditions.

[18]   Gehring, A. and Saal, H., "Yield Strength Distribution in Thin-walled Sections Due to Roll Forming – A Finite-Element Analysis", Proceedings of the 6th International Conference on Steel and Aluminium Structures, Oxford, 2007, pp. 864.

[19]   Box, G.E.P., Hunter, W.G. and Hunter, J.S., "Statistics for Experimenters", 2nd Edition, New York: John Wiley & Sons, 2005.

[20]   Statistica 7.1, Copyright 1986 - 2005, StatSoft, Inc.